Clim. Past Discuss., doi:10.5194/cp-2016-96, 2016
Manuscript under review for journal Clim. Past
Published: 4 October 2016

Climate of the Past Discussions

A chironomid-based mean July temperature inference model from the south-east margin of the Tibetan Plateau, China

Enlou Zhang[a*], Jie Chang[a], Yanmin Cao[b], Hongqu Tang[c], Pete Langdon[d], James Shulmeister[e], Rong Wang[a], Xiangdong Yang[a], Ji Shen[a]

[a] State Key Laboratory of Lake Science and Environment, Nanjing Institute of Geography and Limnology, Chinese Academy of Science, Nanjing 210008, China

[b] College of Resources and Environmental Science, South-Central University for Nationalities, Wuhan 430074, P. R. China

[c] Research Centre of Hydrobiology, Jinan University, Guangzhou 510632, P. R. China

[d] Geography and Environment, University of Southampton, Southampton SO17 1BJ, UK

[e] School of Geography, Planning and Environmental Management, The University of Queensland, St Lucia, Brisbane, Qld 4072, Australia

*Corresponding author Email: elzhang@niglas.ac.cn

Abstract: Chironomid based calibration training sets comprised of 100 lakes from southwestern China and a subset of 47 lakes from Yunnan Province were established. Multivariate ordination analyses were used to investigate the relationship between the distribution of chironomid species and 15 environmental variables from these lakes. Canonical correspondence analyses (CCAs) and partial CCAs showed that mean July temperature is the sole independent and significant ($p < 0.05$) variable that explains 16% of the variance in the chironomid data from the 47 Yunnan lakes. Mean July temperature remains one of the independent and significant variables explaining the second largest amount of variance after potassium ions (K^+) in the 100 south-western Chinese lakes. Quantitative transfer functions were created using the chironomid assemblages for both calibration data sets. The first component of the weighted average partial least square (WA-PLS) model based on the 47 lakes training set produced a coefficient of determination (r^2_{jack}) of 0.83, maximum bias (jackknifed) of 3.15 and root mean squared error of prediction (RMSEP) of 1.72 °C. The two-component WA-PLS model for the 100 lakes training set produced an $r^2_{bootstrap}$ of 0.63, maximum bias (bootstrapped) of 5.16 and RMSEP of 2.31 °C. We applied both transfer functions to a 150-year chironomid record from Tiancai Lake (26°38′3.8 N, 99°43’E, 3898 m a.s.l), Yunnan, China to obtain mean July temperature inferences. The reconstructed results based on both models showed remarkable similarity to each other in terms of pattern. We validated these results by applying several reconstruction diagnostics and comparing them to a 50-year instrumental record from the nearest weather station (26°51'29.22"N, 100°14'2.34"E, 2390 m a.s.l). Both transfer functions perform well in this comparison. We argue that the large training set is also suitable for reconstruction work despite the low explanatory power of MJT because it contains a more complete range of modern temperature and environmental data for the chironomid taxa observed and is therefore more robust.

Clim. Past Discuss., doi:10.5194/cp-2016-96, 2016
Manuscript under review for journal Clim. Past
Published: 4 October 2016

1 Introduction

South-western (SW) China is an important region for examining changes in low and mid-latitudes atmospheric circulation in the Northern Hemisphere (NH). It lies at the intersection of the influence of the NH westerlies and two tropical monsoon systems, namely the Indian Ocean South-west Monsoon (IOSM) and the East Asian Monsoon (EAM) and should be able to inform us about changes in both the latitude and longitude of the influence of these respective systems through time. Reconstructing changes in circulation requires information about several climatic parameters, including past precipitation and temperature. While there are reasonable records of precipitation from this region (e.g. Wang et al., 2001, 2008; Dykoskia et al., 2005; Xiao et al., 2014), there is a paucity of information about temperature changes. In order to understand the extent and intensity of penetration of monsoonal air masses, robust summer temperature estimates are vital as this is the season that the monsoon penetrates SW China.

Chironomid larvae are frequently the most abundant insects in freshwater ecosystems (Cranston, 1995) and subfossil chironomids are widely employed for palaeoenvironmental studies due to their sensitivity to environmental changes and ability of the head capsules to preserve well in lake sediments (Walker, 2001). A strong relationship between chironomid species assemblages and mean summer air temperature have been reported from many regions around the world and transfer functions were subsequently developed (e.g. Brooks and Birks, 2001; Larocque et al., 2001; Heiri et al., 2003; Gajewski et al., 2005; Barley et al., 2006; Woodward and Shulmeister, 2006; Langdon et al., 2008; Rees et al., 2008; Eggermont et al., 2010; Luoto, 2009; Holmes et al., 2011; Heiri et al., 2011; Chang et al., 2015a). The application of these transfer functions has provided quantitative temperature data since the last glacial period in many regions of the world (e.g. Woodward and Shulmeister, 2007; Rees and Cwynar, 2010; Samartin et al., 2012; Chang et al., 2015b; Muschitiello et al., 2015; Brooks et al., 2016). Consequently, subfossil chironomids have been the most widely applied proxy for past summer temperature reconstructions.

Merged regional chironomid training sets and combined inference models have been developed in Europe (Lotter et al., 1999; Holmes et al., 2011; Heiri et al., 2011; Luoto et al., 2014). These large datasets and models provide much more robust reconstructions than smaller local temperature inference models (Heiri et al., 2011; Luoto et al., 2014). However, the distribution of large regional inference models is limited to Europe and northern North America (e.g. Fortin et al., 2015). There is a need to build large training sets for other parts of the world where chironomids will likely be sensitive to temperature changes. Subfossil chironomids have been successfully used as paleoenvironmental indicators in China for over a decade. These included salinity studies on the Tibetan Plateau (Zhang et al, 2007) and the development of a nutrient based inference model for eastern China and parts of

Clim. Past Discuss., doi:10.5194/cp-2016-96, 2016
Manuscript under review for journal Clim. Past
Published: 4 October 2016

Yunnan (Zhang et al., 2006, 2010, 2011, 2012). A large database of relatively undisturbed lakes, in which nutrient changes are minimal while temperature gradients are suitably large, is now available from south-western China and this provides the opportunity to develop a summer temperature inference model for this broad region.

In this study, a chironomid species assemblage training set and a chironomid-based mean July air temperature (MJT) inference model from 100 lakes on south-east margin of the Tibetan Plateau is developed. We also present a 47 lake subset of the training set to provide a local model for Yunnan Province. We compare the output of the two models and evaluate which model is more robust and more suitable for temperature reconstructions in Yunnan. Finally, we test both models by comparing a reconstruction of temperature from Tiancai Lake (26°38′3.8 N, 99°43′E, 3898 m a.s.l) (Fig. 1) in Yunnan Province, SW China for the last 120 years against an instrumental record from Lijiang weather station (26°51'29.22"N, 100°14'2.34"E, 2390 m a.s.l) (Fig. 1), which is the closest meteorological station with a long record.

2 Regional setting

The study area lies in the south-east margin of the Tibetan Plateau including the south-west part of Qinghai Province, the western part of Sichuan Province and the north-west part of Yunnan Province (Fig. 1). It is situated between 26 – 34° N, 99 – 104° E with elevations ranging from about 1000 m to above 5000 m a.s.l.. The 47 lake subset is confined to the north-west part of Yunnan province (Fig. 1) and includes the area around Tiancai Lake.

The study area is characterized by many north-south aligned high mountain ranges (e.g. Hengduan Mountains, Daxue Mountains, Gongga Mountains etc.) that are fault controlled and fall away rapidly into adjacent tectonic basins. The mountain ranges have been deeply dissected by major rivers including the Nujiang, Lancangjiang, Jinshajiang, Yalongjiang and Dadu rivers. Local relief in many places exceeds 3000 m a.s.l..

The climate of the study area is dominated by the westerlies in winter and by the IOSM in Yunnan and Tibet, but some of the easternmost lakes are affected by the EAM. There is a wet season that extends from May (June) to October accounting for 85-90% of total rainfall and a dry season from November to April. Annual precipitation varies greatly according to altitude and latitude. Most of the precipitation is derived from a strong south-west summer monsoonal flow that emanates from the Bay of Bengal (Fig. 1). Precipitation declines from south-east to north-west. Mean summer temperatures vary between about 6 to 22 °C from the north-west to the south-east (Institute of Geography, Chinese Academy of Sciences, 1990). Vegetation across the study area changes from warm temperate to subtropical rainforest at lower elevations in the south-west to alpine grasslands and herb meadows at high altitude.

2.1 Description of model validation site

Tiancai Lake (26°38′3.8 N, 99°43′E, 3898 m a.s.l) (Fig. 1) is in Yunnan Province, on the south-east margin of Tibet Plateau. It is a small alpine lake and has a maximum depth of 7 m, with a water surface area of ~ 2.1 ha and a drainage area of ~3 km^2. Tiancai Lake is dominated in summer by the IOSM, and most likely retains a tropical airflow in winter as the climate is remarkably temperate for this altitude. The mean annual air temperature is approximately 2.5 °C, and the annual precipitation is modelled as 910 mm (Xiao et al. 2014). The lake is charged by 3 streams and directly from precipitation and drains into a lower alpine lake via a stream. The most common rock type in the catchment is a quartz poor granitoid (syenite). Terrestrial vegetation in the catchment consists mainly of conifer forest comprising *Abies* sp. and *Picea* sp. with an understory of *Rhododendron* spp. Above the tree-line, at about 4100 m a.s.l, Ericaceae shrubland (rhododendrons) gives way to alpine herb meadow and rock screes.

3 Methodology

3.1 Field and laboratory analysis

Surface sediment samples were collected from 100 lakes in the south-east margin of the Tibet Plateau via six field campaigns during the autumn of each year between 2006 and 2012. The lakes in this area are mainly distributed at the top or upper slopes of the mountains and are primarily glacial in origin. Most lakes were reached by hiking or with horses and the lake investigation spanned several seasons. Small lakes (surface area c. ~1 km^2) were the primary target for sampling but some larger lakes were also included.

Surface sediments (0-1 cm) were collected from the deepest point in each lake after a survey of the bathymetry using a portable echo-sounder. Surface sediment samples were taken using a Kajak gravity corer (Renberg, 1991). The samples were stored in plastic bags and kept in the refrigerators at 4 °C before analysis. A 30 cm short core was extracted from the centre of Tiancai Lake at a water depth of 6.8 m using UWITEC gravity corer in 2008. The sediment core was sub-sampled at 0.5 cm contiguous intervals and refrigerated at 4°C prior to analysis.

Water samples were collected for chemical analysis from 0.5 m below the lake surface immediately before the sediment samples were obtained. Water samples for chemical analysis were stored in acid-washed polythene bottles and kept at 4 °C until analyses. Secchi depth was measured using a standard transparency disc. Conductivity, pH and dissolved oxygen (DO) were measured in the field using a HI-214 conductivity meter, Hanna EC-214 pH meter and JPB-607 portable DO meter. Chemical variables for the water samples including total phosphorus (TP), total nitrogen (TN), chlorophyll-*a* (chl *a*), K^+, Na^+, Mg^{2+}, Ca^{2+}, Cl^-, SO_4^{2-}, NO_3^- were determined at the Nanjing Institute of Geography and Limnology, Chinese Academy of Sciences. The surface sediments were also analysed for percentage loss-on-ignition (% LOI) following standard methods (Dean 1974). Site-specific values for the mean July air temperature (MJT) and mean annual precipitation (MAP) were estimated using climate layers that were created using statistical downscaling of General Circulation Model (GCM) outputs and terrain parameterization methods in a regular grid network with a grid-cell spacing of 1 km^2 (Böhner 2004, 2006; Böhner and Lehmkuhl, 2005). MJT is used to represent summer temperatures because July is the warmest month in south-western China.

3.2 Chironomid analyses

100 surface sediment samples from lakes of south-western China and 55 sub-samples from the Tiancai Lake short core were analysed for chironomids following standard methods (Brooks et al, 2007). The sediment was deflocculated in 10% potassium hydroxide (KOH) in a water bath at 75 °C for 15 minutes. The samples were then sieved at 212 µm and 90 µm and the residue was examined under a stereo-zoom microscope at x 25. Chironomid head capsules were hand-picked using fine forceps. All the head capsules found were mounted on microscope slides in a solution of Hydromatrix®. Samples produced less than 50 head capsules were not included in the subsequent analyses (Quinlan and Smol, 2001). The chironomid head capsules were identified mainly following Wiederholm (1984), Oliver and Roussel (1982), Rieradevall and Brooks (2001), Brooks et al. (2007) and a photographic guide provided in Tang (2006).

3.3 Numerical analysis

A range of numerical methods were used to determine the relative influence of the measured environmental parameters on the distribution of chironomids in the surface sediments within the training set. A total of fifteen environmental variables were considered in the initial statistical analyses (Table 1). These measurements were normalized using a $\log_{10}$ transformation prior to ordinations following a normality assessment of each data set. Chironomid species were used in the form of square root transformed percentage data in all statistical analyses. The ordinations were performed using CANOCO version 4.5 (ter Braak and Šmilauer, 2002). A detrended correspondence analysis (DCA; Hill and Gauch, 1980) with detrending by segments and nonlinear rescaling was used to explore the chironomid distribution pattern. The DCA was also used to identify the gradient length within the chironomid data and hence whether unimodal analyses were appropriate (ter Braak, 1987). Canonical correspondence analysis (CCA) down-weighted for rare taxa (with a maximum abundance of less than 2% and/or occurred in fewer than two lakes, $N < 2$, $N_2 < 2$), with forward selection and Monte Carlo permutation tests (999 unrestricted permutations) was then used to identify the statistically significant ($p < 0.05$) variables influencing chironomid distribution (ter Braak and Šmilauer, 2002). A preliminary CCA

Clim. Past Discuss., doi:10.5194/cp-2016-96, 2016
Manuscript under review for journal Clim. Past
Published: 4 October 2016

with all fifteen variables was used to identify redundant variables, reducing excessive co-linearity among variables (Hall and Smol, 1992), i.e. the environmental variable with highest variance inflation factor (VIF) was removed after each CCA and the CCA was repeated until all VIFs were less than 20 (ter Braak and Šmilauer, 2002). Only the remaining significant ($p < 0.05$) variables were included in the final CCA ordination. The relationship between significant environmental variables and ordination axes was assessed with canonical coefficients and the associated t-values of the environmental variables with the respective axes. CCA bi-plots of sample and species scores were generated using CanoDraw (ter Braak and Šmilauer, 2002). Partial canonical correspondence analyses (pCCAs) were applied to test the direct and indirect effects of each of the significant variables in relation to the chironomid species data. These were performed for each of the significant variable with and without the remaining significant variables included as co-variables. Environmental variables that retained their significance after all pCCAs were selected for use in the analyses as they are the independent variables.

Chironomid based transfer functions were developed for MJT using C2, version 1.5. (Juggins, 2005). Inference models were developed for the subset of 47 lakes located in Yunnan Province close to or above 4000 m a.s.l. and the full calibration data set of 100 lakes, respectively. The models were constructed using algorithms based on weighted-averaging (WA) and weighted-averaging partial-least-squares (WA-PLS) (Birks, 1995). Jackknifing was applied for the Yunnan calibration data set of 47 lakes as this technique is more robust for data sets with fewer than 80 sites (Kim and Han, 1997). Bootstrap cross-validation technique was tested for the full calibration dataset of 100 lakes as previously demonstrated that it is more suitable for large datasets (Heiri et al., 2011). Transfer function models were evaluated based on the performance of the coefficient of determination (r^2), average bias of predictions, maximum bias of predictions and root mean square error of prediction (RMSEP). The number of components included in the final model was selected based on reducing the RMSEP by at least 5% (Birks, 1998).

The transfer function models based on the 100 full calibration data set and the subset of 47 lakes were then applied to the fossil chironomid data from Tiancai Lake, respectively. MJTs were reconstructed from the site and three types of reconstruction diagnostics suggested in Birks (1995) were applied to assess the reliability of the results. These include goodness-of-fit, modern analogue technique (MAT) and the percentage (%) analysis of modern rare taxa in the fossil samples. For the goodness-of-fit analysis, the squared residual length (SqRL) was calculated by passively fitting fossil samples to the CCA ordination axis of the modern training set data constrained to MJT in CANOCO version 4.5 (ter Braak and Smilauer, 2002). Fossil samples with a SqRL to axis 1 higher than the extreme 10 and 5% of all residual distances in the modern calibration dataset were considered to have a 'poor' and 'very poor' fit with MJT respectively. The chi-square distance to the closest modern assemblage data for each fossil sample was calculated in C2 (Juggins, 2005) using the MAT. Fossil samples with a chi-square distance to the closest modern sample larger than the 5th percentile of all chi-square distances in the modern assemblage data were identified as samples with 'no good' analogue. The percentage of rare taxa in the fossil samples was also calculated in C2 (Juggins, 2005), where a rare taxon has a Hill's $N_2 < 2$ in the modern data set (Hill, 1973). Fossil samples that contain > 10% of these rare taxa were likely to be poorly estimated (Brooks and Birks, 2001). Finally, the chironomid transfer functions inferred MJT patterns were compared to the instrumental recorded data from Lijiang weather station between the years of 1951 and 2014.

3.4. Chronology for Tiancai Lake core

The top 28 cm of the sediment core recovered from Tiancai Lake were used for ^{210}Pb dating. Sediment samples were dated using ^{210}Pb and ^{137}Cs by non-destructive gamma spectrometry (Appleby and Oldfield, 1992). Samples were counted on an Ortec HPGe GWL series well-type coaxial low background intrinsic germanium detector to determine the activities of ^{210}Pb, ^{226}Ra and ^{137}Cs. A total of 58 samples at an interval of every 0.5 cm were prepared and analysed at the Nanjing Institute of Geography and Limnology, Chinese Academy of Sciences. Sediment chronologies were calculated using a composite model (Appleby, 2001). ^{137}Cs was used to identify the 1963 nuclear weapons peak, which was then used as part of a constant rate of supply (CRS) model to calculate a ^{210}Pb chronology for the core.

4 Results

4.1 Distribution of chironomid taxa along the temperature gradient

A total of 53 non-rare taxa ($N > 2$ and $N_2 > 2$) (Brooks and Birks, 2001) chironomid taxa were identified from the 47 Yunnan lakes and a total of 95 non-rare taxa were identified from 100 south-western Chinese lakes (Fig. 2a). Only these non-rare taxa were included in the final transfer function models developed based on the Yunnan subset and full calibration data set respectively. Common cold stenotherms, here defined as taxa with a preference for < 12°C MJT include *Heterotrissocladius marcidus*-type, *Tanytarsus gracilentus*-type, *Paracladius*, *Micropsectra insignilobus*-type, *Micropsectra radialis*-type, *Tanytarsus lugens*-type, *Thienemanniella clavicornis*-type, *Micropsectra* Type A, *Pseudodiamesa*, *Micropsectra atrofasciata*-type and *Corynoneura lobata*-type (Fig. 2a). Taxa characterizing warmer temperatures (> 12°C) include *Polypedilum nubeculosum*-type, *Eukiefferiella gracei*-type, *Microtendipes pedellus*-type and *Tanytarsus lactescens*-type (Fig. 2a). Many of the remaining taxa reflect more cosmopolitan distributions, these include *Procladius*, *Chironomus anthracinus*-type, *Chironomus plumosus*-type, *Corynoneura scutellata*-type, *Tanytarsus pallidicornis*-type, *Tanytarsus mendax*-type and *Paratanytarsus austriacus*-type (Fig. 2a).

Clim. Past Discuss., doi:10.5194/cp-2016-96, 2016
Manuscript under review for journal Clim. Past
Published: 4 October 2016

4.2 Chironomid taxa in Tiancai Lake

A total of 55 sub-samples were analysed for chironomid taxa throughout the top 28 cm of the core recovered from Tiancai Lake. There were 41 non-rare ($N > 2$, $N_2 > 2$) taxa present (Fig. 2b). The general assemblages of these 55 sub-samples include *Heterotrissocladius marcidus*-type, *Tvetenia tamafalva*-type, *Micropsectra insignilobus*-type, *Corynoneura lobata*-type, *Paramerina divisa*-type, *Micropsectra radialis*-type, *Paratanytarsus austriacus*-type, *Thienemanniella clavicornis*-type, *Eukiefferiella claripennis*-type, *Rheocricotopus effusus*-type, *Macropelopia*, *Pseudodiamesa* and *Procladius* (Fig. 2b). All the taxa identified from this record were well represented, and most of them were recognized as cold stenotherms, in the modern calibration training sets (Fig. 2a).

4.3 Ordination analyses and model development

Detrended canonical analyses (DCAs) performed on the 47 lakes from Yunnan showed the gradient length of axis 1 was 3.328, indicating a direct unimodal method was appropriate to model the chironomid species response (Birks 1998). CCAs were then performed on the 47 Yunnan lakes, 53 non-rare taxa and 15 environmental variables. The initial CCA showed total dissolved solids (TDS) had the highest VIF and was removed from further analyses. Among the remaining 14 variables, eight explained a significant ($p < 0.05$) proportion of variance in the chironomid species data (Table 2a, Fig. 3a, b). These were MJT (16%), conductivity (10.7%), K^+ (10.7%), Ca^{2+} (9.9%), TP (5.7%), Cl^- (5.5%), depth (4.4%) and LOI (3.7%). A total of 30.2% variance was explained by the first four CCA axes using the eight significant variables with the first CCA axis explaining nearly half of the total variance. Among these variables, MJT, K^+, depth and Ca^{2+} showed a significant correlation ($p < 0.01$) with CCA axis 1 and Cl^-, MJT, LOI, Ca^{2+} showed a significant correlation ($p < 0.01$) with CCA axis 2 (Table 2a, Fig. 3a, b). MJT explained the largest amount of variance (16%) in the chironomid species data and showed the strongest correlation with CCA axis 1 (Table 2a). The pCCAs results indicated that within the eight significant variables, only MJT retained its significance ($p < 0.01$) after partialling out using pCCAs (Table 3a).

A bi-plot of the CCA species scores indicating the percent of variance explained by the CCA axes in each chironomid taxon with respect to the environmental variables (Fig. 3a). *Microtendipes pedellus*-type, *Einfeldia natchitocheae*-type, *Paratanytarsus penicillatus*-type, *Tanytarsus medax*-type, *Chironomus anthracinus*-type, *Cladopelma edwardsi*-type, *Dicrotendipes nervosus*-type, *Ablabesmyia*, *Tanytarsus pallidicornis*-type, *Procladius*, *Chironomus plumosus*-type, *Cricotopus sylvestris*-type, *Polypedilum nubeculosum*-type, *Tanytarsus lactenscens*-type displayed a substantial amount of variance with the first two CCA axes and were positively correlated with CCA axis 1. These taxa were associated with warm temperatures. *Heterotrissocladius marcidus*-type, *Tanytarsus lugens*-type, *Parametriocnemus*, *Eukiefferiella gracei*-type, *Paramerina divisa*-type and *Micropsectra* type A, showed a negative correlation with

CCA axis 1 and these taxa were inferred as cold temperature indicators. A bi-plot of the CCA sample scores revealed that a large number of sites are closely distributed around depth and LOI, respectively, despite of the low explanatory power of these two variables in the 47 lakes training set (Fig. 3b).

The DCAs performed on the full calibration training set of 100 lakes and 95 non-rare chironomid taxa had an axis 1 gradient length of 3.033 indicating a CCA approach was appropriate for modelling the chironomid taxa response (Birks, 1998). The same 15 environmental variables were tested as in the initial CCA and the results showed that TDS had the highest VIF. It was then removed from the following CCAs. Seven of the remaining 14 variables had significant explanatory power with respect to the chironomid species data. These were K^+ (4.8%), MJT (4.4%), cond (4.4%), Cl^- (3.4%), LOI (3.1%), Na^+ (2.7%) and depth (2%) (Table 2b). A total of 14.6% of variance was explained by the four CCA axes with the 7 significant variables included and the first two axes explained 10% of the total variance. Of these variables, cond and K^+ were significantly correlated ($p < 0.01$) with CCA axis 1 and cond, depth, Cl^-, MJT showed a significant correlation ($p < 0.01$) with CCA axis 2 (Table 2b, Fig. 3a, b). Potassium ions (K^+) explained the largest variance in the chironomid species data and showed the strongest correlation with CCA axis 1. MJT and cond explained equally the second largest amount of variance (4.4%) where MJT was significantly correlated with CCA axis 2 and cond was significantly correlated with both axis 1 and 2 (Table 2b). The pCCAs (Table 3b) demonstrated that within the 7 significant variables K^+, MJT, Cl^-, LOI and depth retained their significance ($p < 0.01$) when the other variables were included as co-variables. Potassium ions (K^+) is the independent variable dominates the first CCA axis. MJT and Cl^- are the independent variables dominating the second CCA axis but MJT has an overall higher explanatory power (Table 2b).

A bi-plot of the CCA species scores indicated that taxa such as *Heterotrissocladius marcidus*-type and *Tanytarsus lugens*-type had a significant amount of variance explained by the first two CCA axes and were negatively correlated with CCA axis 1. Taxa including *Polypedilum nubeculosum*-type, *Chironomus plumosus*-type were positively correlated with CCA axis 1 with a significant amount of variance explained by the CCA axis 1 and 2. A bi-plot of the CCA sample scores showed that a major proportion of sites distributed concentrating around depth (Fig. 3b) whereas depth only explains 2% of the total variance in the 100 lakes calibration dataset.

The transfer functions were developed for mean July temperature (MJT) based on the subset with 47 Yunnan lakes and the full 100 lakes calibration datasets, respectively. We acknowledge that MJT is not the sole independent variable on CCA axis 2 in the 100 lake dataset but transfer functions based on this large regional dataset are created and applied to reconstruct MJT for the purpose of comparing the performance with the more localized Yunnan transfer function models. Both weighted averaging (WA) and weighted averaging partial least squares (WA-PLS) models were tested for MJT in the respective modern calibration sets. Summary statistics of inference models based on these two different numerical methods are listed in Table 4. The WA with inverse deshrinking (WAinv) and WA-PLS models generated similar statistical results for both calibration training sets. For the subset of 47 Yunnan lakes, the WAinv model produced a strong jackknifed coefficient of determination (r^2_{jack}) of 0.83, average bias (AveBiasjack) of 0.113, maximum bias (MaxBiasjack) of 2.83 and root mean squared error of prediction (RMSEP) of 1.67 °C (Table 4a). The first component of WA-PLS model was selected and it produced the same r^2_{jack} of 0.83, AveBiasjack of 0.109, a slightly higher MaxBiasjack of 3.15 and RMSEP of 1.72 °C (Table 4a). Fig. 4a and 4b show the chironomid-inferred versus observed MJT and the distribution of prediction residuals for the transfer function models based on the subset of 47 lakes from Yunnan.

For the full calibration set of 100 south-western Chinese lakes, bootstrap cross-validation techniques was applied for both the WAinv and WA-PLS models (Table 4). Similar to the Yunnan subset, the WAinv and WA-PLS model produced comparable statistical results. The WAinv model produced an r^2_{boot} of 0.61, AveBiasboot of 0.06, MaxBiasboot of 5.30 and RMSEP (s1 + s2) of 2.30 °C (RMSEs1 = 0.69 °C and RMSEs2 = 2.19 °C) (Table 4a). We selected the second component of WA-PLS bootstrap model as it is the most robust and reduced the RMSEP by more than 5%. It produced an r^2_{boot} of 0.63, AveBiasboot of 0.101**,** a lower MaxBiasboot of 5.16 and RMSEP (s1 + s2) of 2.31 °C (RMSEs1 = 0.89 °C and RMSEs2 = 2.14 °C). Fig. 4c and 4d show the chironomid-inferred versus observed MJT and the distribution of prediction residuals for the transfer function models based on the full calibration training set of 100 lakes.

4.4 Reconstructions from Tiancai Lake

The ^{210}Pb dating results demonstrated that the top 28 cm of the short core recovered from Tiancai Lake represent the last c. ~150 years (Fig 5). We applied all four new transfer function models (WA-47 lakes, WA-100 lakes, WAPLS-47 lakes, WAPLS-100 lakes) to reconstruct the MJT changes between 1860 AD and 2008 (Fig. 6a). The WA and WA-PLS models constructed based on the subset of Yunnan lakes and the full calibration dataset 100 lakes showed identical trends in the MJT reconstructions over the last c. ~150 years (Fig. 6a). There were small deviations in terms of absolute values but the variations in the reconstructed MJT among the four models were within 0-0.5 °C for each sample (Fig. 6a). Goodness-of-fit analysis on the reconstruction results based on the 100 lake dataset showed that out of the 55 fossil samples, eight samples from the years between 2000 and 2007 AD have ‘poor’ and ‘very poor’ fit to MJT (Fig. 6b). The modern analogue analysis showed that only four fossil samples have ‘no good’ analogues in the 100 lake dataset (Fig. 6c). All 55 fossil samples contain less than 10% of the taxa that were rare in the modern 100 lake training set (Fig. 6d). Finally, the reconstructed results also showed a comparable MJT trend with the instrumental measured data between 1951 and 2007 AD from Lijiang weather station (Fig. 6e).

Clim. Past Discuss., doi:10.5194/cp-2016-96, 2016
Manuscript under review for journal Clim. Past
Published: 4 October 2016

5 Discussion

5.1 Reliability of the environmental and chironomid data

Obtaining reliable estimates of the modern climate data has been challenging in south-western China. There are very few meteorological stations and climate monitoring in the high mountains of our study area is virtually non-existent. Climate parameters including MJT and mean annual precipitation used in this study are interpolated from climate surfaces derived from a mathematical climate surface model based on the limited meteorological data and a digital terrain model (DTM) applied to the whole of the wider Tibetan region (4000 x 3000 km) (Böhner, 2006). We acknowledge that there are limitations in these data due to the sparse distribution of observations from meteorological stations. Modelling precipitation in topographically complex parts of this region such as the Yunnan is problematic due to the orographic interception (or non-interception) of monsoonal air masses upwind of the sites, but the scale of the DTM means that mean temperature data should be reasonably robust, except in the most topographically complex areas. Further meteorological observations are required to refine this and other studies.

We examined the chironomid taxa that appeared as temperature indicators in the 47 and 100 lake datasets respectively. A number of taxa, namely *Diamesa*, *Parametriocnemus* and *Tvetenia tamafalva*-type emerge as cold stenotherms in the 47 lake dataset but not in the 100 lake dataset. *Diamesa*, *Parametriocnemus* and *Tvetenia tamafalva*-type displayed a more cosmopolitan distribution in the larger training set. We further examined these taxa and we identified that *Diamesa*, *Parametriocnemus* and *Tvetenia tamafalva*-type are all lotic (Cranston, 2010). These taxa would likely have washed in to the lakes from streams and therefore it is not appropriate to make temperature inferences based on them. While they appeared as cold stenotherms in the 47 lakes dataset, it is mainly because this training set had lakes with limited in flows except in the alpine lakes. This created the impression of these taxa being cold stenotherms whereas the inclusion of additional lowland lakes that had stream inflows in the larger data set allowed the identification of this misrepresentation. In summary, the 100 lake training set has allowed better identification of environmental tolerance of chironomid taxa in the south-western China data sets.

5.2 Comparison of environmental gradients between the 47 and 100 lakes datasets

The training set, comprising 47 lakes in Yunnan covers MJTs between 5.6 °C and 18.8 °C and yields a MJT gradient of 13.2 °C. The ordination analyses (CCAs and pCCAs) of this dataset showed that MJT is the only independent variable on CCA axis 1 and explained the largest amount of the total variance (16%) in the chironomid data. Based on these statistical results, the 47 Yunnan lake training set initially appeared

Clim. Past Discuss., doi:10.5194/cp-2016-96, 2016
Manuscript under review for journal Clim. Past
Published: 4 October 2016

more appropriate for developing a MJT chironomid-based transfer function (Juggins, 2013).

The 100 lake training set covers a longer temperature gradient ranging from 4.2 °C to 20.8 °C (MJT gradient of 16.6 °C). Based on the CCAs, we observed that the MJT signal in this larger training set is partially masked by a salinity gradient. This is represented by potassium ions (K^+) and conductivity (Fig. 3c, d). CCA axis 1 is dominated by K^+ and this may be related to weak weathering. This is because (1) the first CCA axis is driven by lakes that have low precipitation but intermediate level of evaporation, examples of these sites include Lake Xiniuhaijiuzhai, Lake Muchenghai and Lake Kashacuo, from the north margin of Sichuan Province. These lakes indicate cool, dry and low windiness conditions that lead to a weak weathering environment. We highlight that this area is different from the high Tibetan Plateau where aridity and salinity dominates. (2) In chemical weathering sequences, K^+ is an early stage weathering product (Meunier and Velde, 2013) and K^+ is often associated with primary minerals, such as feldspars and micas in the bedrock (Hinkley, 1996). Salinity is responding to both temperature and aridity but further pCCAs indicate that both K^+ and MJT are independent variables in this training set.

The second CCA axis is co-dominated by MJT and Cl^- with very similar gradient lengths. Lakes distributed along the warmer end of the MJT gradient include Lake Longtan, Lake Lutu, Lake Luoguopingdahaizi and Lake Jianhu. Most of these sites are lower to intermediate altitude sites in the dataset (below 2700 m a.s.l) because elevation is correlated with temperature. Sodium ions (Na^+) largely follow the same axis as MJT as evaporation is related in part to temperature. In summary, MJT and Cl^- are both independent variables that drive the second CCA axis and Cl^-, and Na^+ partially reflect evaporation effects because, on average, lakes in warmer climates evaporate more than those in colder ones. In addition, Cl^- concentration may also relate to the characteristics of the bedrock geology of the region. We highlight that there are very few lakes on the Cl^- gradient and these lakes are from the border of Sichuan and Yunnan Provinces, where geothermal springs are widespread. We argue that developing a MJT transfer function is appropriate for the 100 lake training set because MJT is independent of other variables (e.g. Rees et al., 2008; Chang et al., 2015a). Although Cl^- is also independent and co-dominates CCA axis 2, the overall explanatory power is lower (Table 2b) and also the lambda ratio ($\lambda1/\lambda2$) is less than MJT (Table 3b). We retained all 100 lakes from the region without removing sites to artificially enhance the MJT gradient in the ordination analyses and model development because this 100 lake dataset is a more accurate reflection of the natural environment of SW China.

We re-highlight that some chironomid taxa appeared as stenotherms in the 47 lake dataset only because the dataset does not cover the full environmental range. For example, the CCA bi-plot for the 47 lake training set indicating that *Tanytarsus gracilentus*-type, *Tvetenia tamafalva*-type and *Micropsectra* follow the MJT gradient

Clim. Past Discuss., doi:10.5194/cp-2016-96, 2016
Manuscript under review for journal Clim. Past
Published: 4 October 2016

closely (Fig 3a). In the 100 lake training set, we observed that *Tanytarsus gracilentus*-type is more closely related to lake depth, while both *Tvetenia tamafalva*-type and *Micropsectra* show closer correlation with LOI and Cl^- instead of MJT. The latter observations match with the ecological recognition and interpretation of these taxa in literature where *Tanytarsus gracilentus*-type was identified as a benthic species in the arctic (Einarsson et al., 2004; Ives et al., 2008); *Tvetenia tamafalva*-type was often found in streams and this is likely related to the organic content (LOI) of the substrates as they are detritus feeders (Brennan and McLachlan, 1979); while *Micropsectra* was found in thermal springs and pools (Hayford et al., 1995; Batzer and Boix, 2016) and this is reflected in this dataset with having a close relationship with Cl^-. It presents in lakes such as Lake Tengchongqinghai, Qicai Lake and Lake Haizibian that have high levels of Cl^- ions. These sites are located in geothermal spring region of Sichuan and Yunnan Provinces.

Well-known warm stenotherms that are distributed along the MJT gradient of the CCA species bi-plot (Fig. 3c) for the 100 dataset include *Dicrotendipes*, *Microchironomus*, *Polypedilum* and *Microtendipes*. Many studies (e.g. Walker et al. 1991; Larocque et al. 2001; Rosenberg et al., 2004; Brodersen and Quinlan, 2006; Woodward and Shulmeister, 2006) show that these taxa are warm temperature indicators worldwide. We therefore further argue that while MJT explained a higher total variance in the chironomid data in the 47 Yunnan lake training set, the 100 lake training set has a clear advantage in that it contains a more complete range of temperatures and environments expected to have been experienced by lakes and their chironomid fauna in the past (Brooks and Birks, 2001). This will be particularly useful when applying the models to reconstruct changes in the late Pleistocene and Holocene when climates were different (Heiri et al., 2011).

5.3 Comparisons of the transfer function statistics

We compared the statistical results of the transfer functions generated from the 47 and 100 lakes training sets. We selected the WA-PLS based models over the WAinv based approach for both training sets because the addition of PLS components can reduce the prediction error in datasets with moderate to large noise (ter Braak and Juggins, 1993). The 47 lake dataset WA-PLS model yields a strong r^2_{jack} (0.83) and a comparably lower $RMSEP_{jack}$ (1.7 °C, represents 12.8% of scalar length of the MJT gradient). The performance of the model is highly comparable to models of a similar kind worldwide such as from eastern North America with 136 lakes (r^2 = 0.82, Barley et al., 2006) and Finland with 77 lakes (r^2 = 0.78, Luoto, 2009) where the RMSEPs represent 11.7% and 12.5% of their respective temperature gradient length. However, there are apparent caveats in the distribution of the model predicted MJTs and error residuals along the temperature gradient (Fig.4a-d). These include: (1) there is a gap in sites between the MJTs of 12 and 15 °C; (2) there is a wide scatter of error residuals for sites located in an intermediate temperature range (between 10 and 12 °C) and at the warmer end (> 18 °C). These indicate there are limitations for the model to accurately reconstruct temperatures in warmer conditions (e.g. the Holocene) and during relatively minor cooling events (e.g. the Little Ice Age). The 47 lakes training set covers a MJT gradient of 13.2 °C and this should be capable of detecting glacial to interglacial changes. The problem in the smaller data set is that some taxa are likely to have their climate tolerances and optima significantly underestimated (Heiri et al., 2011). For example, *Diamesa*, is present up to a MJT of 10 °C in the 47 lake dataset, whereas in the 100 lake dataset, it is present in samples with a MJT of 17 °C. The consequence of this is that *Diamesa* appears as a cold stenotherm in the 47 lakes dataset but it is actually cosmopolitan. This finding is in line with Heiri et al. (2011) and Brooks and Birks (2001), who demonstrated from Europe that broader datasets give a more accurate view of the chironomid distribution data.

The 100 lakes training set extends the MJT gradient by 3.4 °C to 16.6 °C and the RMSEP represents 13.8% of the scalar length of the MJT gradient. This is still comparable with most chironomid transfer function models including transfer function models developed from Northern Sweden with 100 lakes (r^2 = 0.65, Larocque et al., 2001) and western Ireland with 50 lakes (r^2 = 0.60, Potito et al., 2014), representing 14.7% and 15% of the scaler length of the temperature gradient respectively. Despite of the relatively lower model coefficient (r_{boot} = 0.63), we observe that by increasing the number of lakes in the calibration set, the distribution of the sites along the MJT gradient is evened out (Fig. 4d). The distribution of the error residuals generates a smoother curve (Fig. 4d) than the 47 lakes training set. The model leads to overestimation of low and underestimation of high temperature values which is typical of the WA models (ter Braak and Juggins, 1993). We acknowledge that the lower model coefficient (r_{boot}) may relate to the lowered explanatory power of MJT in the chironomid species data and increased number of independent and significant variables in the 100 lake training set when a wider range of lakes were included. However, increasing the length of the temperature gradient allowed the incorporation of full potential abundance and distributional ranges for each of the chironomid taxa.

5.4 Tiancai Lake reconstructions

The 47 lakes training set displays an apparently stronger statistical correlation to the temperature record. We argue that the increased robustness of applying the transfer function model based on the larger dataset outweigh the modest reduction in statistical performance. All three types of diagnostic techniques applied (Fig 6 b-d) suggest that a reliable MJT reconstruction was provided by the WAPLS model based on the 100 lake dataset overall. We also predict that the model based on the larger dataset may amplify both cool and warm events because it covers a more complete environmental range, allowing taxon responses to be fully observed. In order to test this and also to test whether either reconstruction matches reality, we applied both of the WAPLS models to the Tiancai Lake chironomid data, for the period between 1860 AD and the present.

Clim. Past Discuss., doi:10.5194/cp-2016-96, 2016
Manuscript under review for journal Clim. Past
Published: 4 October 2016

We plot the trends of MJT reconstruction results from both the WAPLS models against the ~50-year long instrumental record from Lijiang station (Fig. 6e). We do not expect the absolute MJT values to be identical because Lijiang is located ~55 km east-northeast (ENE) and ~1600 m lower in altitude than Tiancai Lake. We applied a typical environmental lapse rate of temperature (change with altitude) for Alpine regions, which is 0.58 °C per 100 metres (Rolland, 2003) to estimate the equivalent MJT values from Lijiang station. If the chironomid based transfer functions are able to provide reliable estimates for MJTs, we expect the records demonstrate a similar trend with the instrumental data (Fig. 6e).

The reconstruction results are well matched with the expected outcomes: (1) It is reassuring that the transfer function model based on 100 lakes dataset for a broader area of SW China reconstructs mean July temperatures (MJTs) with a similar pattern to the 47 Yunnan lakes dataset in terms of the trend; (2) as expected, the WAPLS model based on the 100 dataset amplifies both cool and warm periods; (3) both chironomid based reconstructions broadly match the trend recorded by the instrument. By applying the environmental lapse rate, we observe a temperature depression from Lijiang to Tiancai Lake of about 9.3 °C (giving an inferred MJT at Tiancai Lake of 8.4°C). This magnitude of change is consistent with the reconstructions from Tiancai Lake, where the difference in mean is 0.67 °C (equivalent to a MJT of 7.7 °C) when compared to the results derived from the 100 lake based WAPLS model and 0.86 °C (equivalent MJT of 7.5 °C) for the 47 lake model. The implication is that the 100 lake based model may be able to reconstruct the MJTs that better reflect the actual climate record, though the difference between the models is small. We observe there are minor out of phase patterns and this may reflect the uncertainties of applying the ^{210}Pb chronology to very recent lake sediments (Binford, 1990). Furthermore, we note that sediment samples reflect more than one season and consequently the total range of the temperature reconstructions from the chironomid samples is likely to be slightly less than the meteorological data because of the smearing out of extreme years. While we expect overall trends between Lijiang and Tiancai Lake to be similar, the sites are not closely co-located and some natural variability between the sites is expected. A significant correlation ($p < 0.05$, $r = 0.45$, $n = 31$) was still obtained between the instrumental data and the 100 lake WAPLS model inferred MJT data for the last ~ 50 years. In summary, the WAPLS model based on the 100 lake chironomid training set has produced reliable summer temperature records and can realistically also be applied to reconstructing past climate in SW China.

6 Conclusions

Two chironomid based summer temperature transfer functions have been constructed and applied to Yunnan region in SW China. These include transfer functions based on a 47 lakes training set confined to Yunnan and a 100 lakes training set from a broader region of south-western China. The first component of WA-PLS model based on the 47 lakes training set produced an r^2_{jack} of 0.83, AveBiasjack of 0.11, a MaxBiasjack of

3.15 and RMSEP of 1.72 °C. The second component of WA-PLS bootstrap model for the 100 lakes training set is the most robust for those data and produced an r^2_{boot} of 0.63, AveBiasboot of 0.10**,** a MaxBiasboot of 5.16 and RMSEP (s1 + s2) of 2.31 °C (whereas RMSEs1 = 0.88 °C and RMSEs2 = 2.14 °C). Both the ordination and transfer function statistics show that the 47 lakes training set has a stronger correlation with MJT, but in practice, we demonstrated that the reconstruction results based on the 100 lakes training set are also reliable. The larger dataset may potentially provide a better representation of the environmental preferences of the chironomid taxa. The 100 lakes training set allowed insight into chironomid distribution despite having many more independent environmental gradients. The test of the two transfer function models against the modern data suggest that the WA-PLS models provided near identical reconstructions that match the trend of the local instrumental record for the last 50 years. As also demonstrated from pan-European chironomid based transfer functions (e.g. Brooks and Birks, 2001; Heiri et al., 2011), the broadly based 100 SW Chinese lakes is likely more robust and is equally appropriate for use reconstructing long-term summer temperature changes of SW China**.**

Acknowledgement: We thank X Chen, E.F. Liu, M. Ji, R. Chen, Y.L. Li, J.J. Wang, Q. Lin and B.Y. Zheng (Nanjing Institute of Geography and Limnology, Chinese Academy of Sciences) for field assistance, Jürgen Böhner (Georg-August-University Göttingen, Germany) for help with climate data, This research was supported by the Program of Global Change and Mitigation (2016YFA0600502), the National Natural Science Foundation of China (No. 41272380, 41572237).

Clim. Past Discuss., doi:10.5194/cp-2016-96, 2016
Manuscript under review for journal Clim. Past
Published: 4 October 2016

References

Appleby, P.G., 2001.Chronostratigraphic techniques in recent sediment, In: Last WM, Smol J P. Tracking environmental change using lake sediments, Volume 1: basin analysis, coring, and chronological techniques. Klauwer Academic Publishers, pp. 171-196.

Appleby, P.G., Oldfield, F., 1992. Application of 210Pb to sedimentation studies. In: Ivanovich M, Harmon RS (Eds.), Uranium series disequilibrium. OUP, pp. 731-778.

Batzer, D., Boix, D., 2016. Invertebrates in Freshwater Wetlands: An International Perspective on their Ecology. Springer. pp. 361 – 370.

Barley, E.M., Walker, I.R., Kurek, J., Cwynar, L.C., Mathewes, R.W., Gajewski, K., Finney, B.P., 2006. A northwest North American training set: Distribution of freshwater midges in relation to air temperature and lake depth. Journal of Paleolimnology 36, 295-314

Binford, M.W., 1990. Calculation and uncertainty analysis of 210Pb dates for PIRLA project lake sediment cores. Journal of Paleolimnology 3, 253-267.

Birks, H.J.B., 1998. Numerical tools in paleolimnology progress, potentialities, and problems. Journal of Paleolimnology 20, 307–332.

Birks, H.J.B., 1995. Quantitative palaeoenvironmental reconstructions. In: Maddy, D., Brew, J.S. (Eds.), Statistical Modelling of Quaternary Science Data. Technical Guide 5. Quaternary Research Association, Cambridge, pp. 116–254

Böhner, J., 2006. General climatic controls and topoclimatic variations in Central and High Asia. Boreas 35, 279-295.

Böhner, J., Lehmkuhl, F., 2005. Environmental change modelling for Central and High Asia: Pleistocene, present and future scenarios. Boreas 34, 220-231.

Brennan, A., McLachlan, A.J., 1979. Tubes and tube-building in a lotic Chironomid (Diptera) community. Hydrobiologia 67, 173-178.

Brodersen, K.P., Quinlan, R., 2006. Midges as palaeoindicators of lake productivity, eutrophication and hypolimnetic oxygen. Quaternary Science Reviews 25, 1995-2012.

Brooks, S.J., Birks, H.J.B., 2001. Chironomid-inferred air temperatures from Lateglacial and Holocene sites in north-west Europe: progress and problems. Quaternary Science Reviews 20, 1723-1741.

Brooks, S.J., Davies, K.L., Mather, K.A., Matthews, I.P., Lowe, J.J., 2016. Chironomid-inferred summer temperatures for the Last Glacial–Interglacial Transition from a lake sediment sequence in Muir Park Reservoir, west-central Scotland. Journal of Quaternary Science 31, 214-224.

Brooks, S.J., Langdon, P.G., Heiri, O., 2007. The Identification and Use of Palaearctic Chironomidae Larvae in Palaeoecology. Quaternary Research Association.

Chang, J.C., Shulmeister, J., Woodward, C., 2015. A chironomid based transfer function for reconstructing summer temperatures in southeastern Australia. Palaeogeography, Palaeoclimatology, Palaeoecology 423, 109-121.

Chang, J.C., Shulmeister, J., Woodward, C., Steinberger, L., Tibby, J., Barr, C., 2015. A chironomid-inferred summer temperature reconstruction from subtropical Australia

Clim. Past Discuss., doi:10.5194/cp-2016-96, 2016
Manuscript under review for journal Clim. Past
Published: 4 October 2016

Climate of the Past Discussions

during the last glacial maximum (LGM) and the last deglaciation. Quaternary Science Reviews 122, 282-292.

Cranston. P.S., 1995. Chironomids: from Genes to Ecosystems, CSIRO, Melbourne, pp. 482.

Cranston, P.S., 2000. Electronic guide to the chironomidae of Australia. http://www.science.uts.edu.au/sasb/chiropage/

Dean Jr, W.E., 1974. Determination of carbonate and organic matter in calcareous sediments and sedimentary rocks by loss on ignition: comparison with other methods. Journal of Sedimentary Research, 44, 242-248.

Dykoski, C.A., Edwards, R.L., Cheng, H., Yuan, D., Cai, Y., Zhang, M., Lin, Y., Qing, J., An, Z., Revenaugh, J., 2005. A high-resolution, absolute-dated Holocene and deglacial Asian monsoon record from Dongge Cave, China. Earth and Planetary Science Letters 233, 71-86.

Eggermont, H., Heiri, O., Russell, J., Vuille, M., Audenaert, L., Verschuren, D., 2010. Paleotemperature reconstruction in tropical Africa using fossil Chironomidae (Insecta: Diptera). Journal of Paleolimnology 43, 413-435.

Einarsson, Á., Stefánsdóttir, G., Jóhannesson, H., Ólafsson, J.S., Már Gíslason, G., Wakana, I., Gudbergsson, G., Gardarsson, A., 2004. The ecology of Lake Myvatn and the River Laxá: Variation in space and time. Aquatic Ecology 38, 317-348.

Fortin, M.C., Medeiros, A.S., Gajewski, K., Barley, E.M., Larocque-Tobler, I., Porinchu, D.F., Wilson, S.E., 2015. Chironomid-environment relations in northern North America. Journal of Paleolimnology 54, 223-237.

Gajewski, K., Bouchard, G., Wilson, S.E., Kurek, J., Cwynar, L.C., 2005. Distribution of Chironomidae (Insecta: Diptera) Head Capsulesin Recent Sediments of Canadian Arctic Lakes. Hydrobiologia 549, 131-143.

Hall, R.I., Smol, J.P., 1992. A weighted—averaging regression and calibration model for inferring total phosphorus concentration from diatoms in British Columbia (Canada) lakes. Freshwater Biology 27, 417-434.

Hayford, B.L., Sublette, J.E., Herrmann, S.J., 1995. Distribution of Chironomids (Diptera: Chironomidae) and Ceratopogonids (Diptera: Ceratopogonidae) along a Colorado Thermal Spring Effluent. Journal of the Kansas Entomological Society 68, 77-92.

Heiri, O., Brooks, S.J., Birks, H.J.B., Lotter, A.F., 2011. A 274-lake calibration data-set and inference model for chironomid-based summer air temperature reconstruction in Europe. Quaternary Science Reviews 30, 3445-3456.

Heiri, O., Lotter, A.F., Hausmann, S., Kienast, F., 2003. A chironomid-based Holocene summer air temperature reconstruction from the Swiss Alps. The Holocene 13, 477-484.

Hill, M.O., Gauch, H.G., 1980. Detrended Correspondence Analysis: An Improved Ordination Technique. Vegetatio 42, 47–58.

Hinkley, T.K., 1996. Preferential Weathering of Potassium Feldspar in Mature Soils, Earth Processes: Reading the Isotopic Code. American Geophysical Union, pp. 377-389.

Holmes, N., Langdon, P.G., Caseldine, C., Brooks, S.J., Birks, H.J.B., 2011. Merging chironomid training sets: implications for palaeoclimate reconstructions. Quaternary Science Reviews 30, 2793-2804.

Ives, A.R., Einarsson, A., Jansen, V.A.A., Gardarsson, A., 2008. High-amplitude fluctuations and alternative dynamical states of midges in Lake Myvatn. Nature 452, 84-87.

Kim, N., Han, J.K., 1997. Assessing the integrity of cross-validation: a case for small sample-based research. Hong Kong University of Science and Technology, Department of Marketing, Working Paper Series no. MKTG 97.096

Langdon, P.G., Holmes, N., Caseldine, C.J., 2008. Environmental controls on modern chironomid faunas from NW Iceland and implications for reconstructing climate change. Journal of Paleolimnology 40, 273-293.

Larocque, I., Hall, R.I., Grahn, E., 2001. Chironomids as indicators of climate change: a 100-lake training set from a subarctic region of northern Sweden (Lapland). Journal of Paleolimnology 26, 307-322.

Lotter, A.F., Walker, I.R., Brooks, S.J., Hofmann, W., 1999. An intercontinental comparison of chironomid palaeotemperature inference models: Europe vs North America. Quaternary Science Reviews 18, 717-735.

Luoto, T.P., 2009. A Finnish chironomid- and chaoborid-based inference model for reconstructing past lake levels. Quaternary Science Reviews 28, 1481-1489.

Luoto, T.P., Kaukolehto, M., Weckström, J., Korhola, A., Väliranta, M., 2014. New evidence of warm early-Holocene summers in subarctic Finland based on an enhanced regional chironomid-based temperature calibration model. Quaternary Research 81, 50-62.

Institute of Geography, Chinese Academy of Sciences, 1990. Atlas of Tibet Plateau. Science Press. (in Chinese).

Juggins, S., 2005. C2 Version 1.5: software for ecological and palaeoecological data analysis and visualisation. University of Newcastle, Newcastle-upon-Tyne.

Juggins, S., 2013. Quantitative reconstructions in palaeolimnology: new paradigm or sick science? Quaternary Science Reviews 64, 20-32.

Meunier, A. and Velde, B.D., 2013. Illite: Origins, evolution and metamorphism. Springer Science & Business Media, pp. 65 – 76.

Muschitiello, F., Pausata, F.S.R., Watson, J.E., Smittenberg, R.H., Salih, A.A.M., Brooks, S.J., Whitehouse, N.J., Karlatou-Charalampopoulou, A., Wohlfarth, B., 2015. Fennoscandian freshwater control on Greenland hydroclimate shifts at the onset of the Younger Dryas. Nature Communications 6.

Oliver, D.R., Roussel, M.E. 1982. The larvae of Pagastia Oliver (Diptera: Chironomidae) with descriptions of three new species. The Canadian Entomologist, 114: 849–854.

Potito, A.P., Woodward, C.A., McKeown, M., Beilman, D.W., 2014. Modern influences on chironomid distribution in western Ireland: potential for palaeoenvironmental reconstruction. Journal of Paleolimnology 52, 385-404.

Quinlan, R., Smol, J.P., 2001. Setting minimum head capsule abundance and taxa deletion criteria in chironomid-based inference models. Journal of Paleolimnology 26, 327-342.

Clim. Past Discuss., doi:10.5194/cp-2016-96, 2016
Manuscript under review for journal Clim. Past
Published: 4 October 2016

Rees, A.B.H., Cwynar, L.C., 2010. Evidence for early postglacial warming in Mount Field National Park, Tasmania. Quaternary Science Reviews 29, 443-454.

Rees, A.B.H., Cwynar, L.C., Cranston, P.S., 2008. Midges (Chironomidae, Ceratopogonidae, Chaoboridae) as a temperature proxy: a training set from Tasmania, Australia. Journal of Paleolimnology 40, 1159-1178.

Renberg, I., 1991. The HON-Kajak sediment corer. Journal of Paleolimnology 6, 167-170.

Rieradevall, M., Brooks, S.J., 2001. An identification guide to subfossil Tanypodinae larvae (Insecta: Diptera: Chrironomidae) based on cephalic setation. Journal of Paleolimnology 25, 81-99.

Rolland, C., 2003. Spatial and Seasonal Variations of Air Temperature Lapse Rates in Alpine Regions. Journal of Climate 16, 1032-1046.

Rosenberg, S.M., Walker, I.R., Mathewes, R.W., Hallett, D.J., 2004. Midge-inferred Holocene climate history of two subalpine lakes in southern British Columbia, Canada. The Holocene 14, 258-271.

Samartin, S., Heiri, O., Vescovi, E., Brooks, S.J., Tinner, W., 2012. Lateglacial and early Holocene summer temperatures in the southern Swiss Alps reconstructed using fossil chironomids. Journal of Quaternary Science 27, 279-289.

Tang, H. Q. 2006. Biosystematic study on the chironomid larvae in China (Diptera: Chironomidae). Nankai University, Tianjin, China, 945pp.

ter Braak, C. J. F., 1987. Unimodal models to relate species to environment. Agricultural Mathematics Group, Wageningen, The Netherlands. pp. 152

ter Braak, C.J.F., Juggins, S., 1993. Weighted averaging partial least squares regression (WA-PLS): an improved method for reconstructing environmental variables from species assemblages. Hydrobiologia 269, 485-502.

ter Braak, C.J.F., Šmilauer, P., 2002. CANOCO reference manual and CanoDraw for Windows user's guide: software for canonical community ordination (version 4.5), Microcomputer power, Itaca, www.canoco.com.

Walker, I. R., 2001. Midges: Chironomidae and related Diptera. In: J. P. Smol, H. J. B. Birks, and W. M. Last (Eds), Tracking Environmental Change Using Lake Sediments. Volume 4. Zoological Indicators. Kluwer Academic Publishers, Dordrecht. pp. 43-66.

Walker, I.R., Smol, J.P., Engstrom, D.R., Birks, H.J.B., 1991. An Assessment of Chironomidae as Quantitative Indicators of Past Climatic Change. Canadian Journal of Fisheries and Aquatic Sciences 48, 975-987.

Wang, Y.J., Cheng, H., Edwards, R.L., An, Z.S., Wu, J.Y., Shen, C.C., Dorale, J.A., 2001. A High-Resolution Absolute-Dated Late Pleistocene Monsoon Record from Hulu Cave, China. Science 294, 2345-2348.

Wang, Y., Cheng, H., Edwards, R.L., Kong, X., Shao, X., Chen, S., Wu, J., Jiang, X., Wang, X., An, Z., 2008. Millennial- and orbital-scale changes in the East Asian monsoon over the past 224,000 years. Nature 451, 1090-1093.

Wiederholm, T., 1984. Incidence of deformed chironomid larvae (Diptera: Chironomidae) in Swedish lakes. Hydrobiologia 109, 243-249.

Woodward, C.A., Shulmeister, J., 2006. New Zealand chironomids as proxies for human-induced and natural environmental change: Transfer functions for temperature and lake production (chlorophyll a). Journal of Paleolimnology 36, 407-429.

Woodward, C.A., Shulmeister, J., 2007. Chironomid-based reconstructions of summer air temperature from lake deposits in Lyndon Stream, New Zealand spanning the MIS 3/2 transition. Quaternary Science Reviews 26, 142-154.

Xiao, X., Haberle, S.G., Shen, J., Yang, X., Han, Y., Zhang, E., Wang, S., 2014. Latest Pleistocene and Holocene vegetation and climate history inferred from an alpine lacustrine record, northwestern Yunnan Province, southwestern China. Quaternary Science Reviews 86, 35-48.

Zhang, E., Bedford, A. Jones,R., Shen, J., Wang, S., Tang, H., 2006. A subfossil chironomid-total phosphorus inference model from the middle and lower reaches of Yangtze River lakes. Chinese Science Bulletin. 51: 2125-2132

Zhang, E., Cao, Y., Langdon, P., Jones, R., Yang, X., Shen, J., 2012. Alternate trajectories in historic trophic change from two lakes in the same catchment, Huayang Basin, middle reach of Yangtze River, China. Journal of Paleolimnology 48, 367-381.

Zhang, E., Jones, R., Bedford, A., Langdon, P., Tang, H., 2007. A chironomid-based salinity inference model from lakes on the Tibetan Plateau. Journal of Paleolimnology 38, 477-491.

Zhang, E., Langdon, P., Tang, H., Jones, R., Yang, X., Shen, J., 2011. Ecological influences affecting the distribution of larval chironomid communities in the lakes on Yunnan Plateau, SW China. Fundamental and Applied Limnology 179, 103-113.

Zhang, E., Liu, E., Jones, R., Langdon, P., Yang, X., Shen, J., 2010. A 150-year record of recent changes in human activity and eutrophication of Lake Wushan from the middle reach of the Yangze River, China. Journal of Limnology 69, 235-241.

Clim. Past Discuss., doi:10.5194/cp-2016-96, 2016
Manuscript under review for journal Clim. Past
Published: 4 October 2016

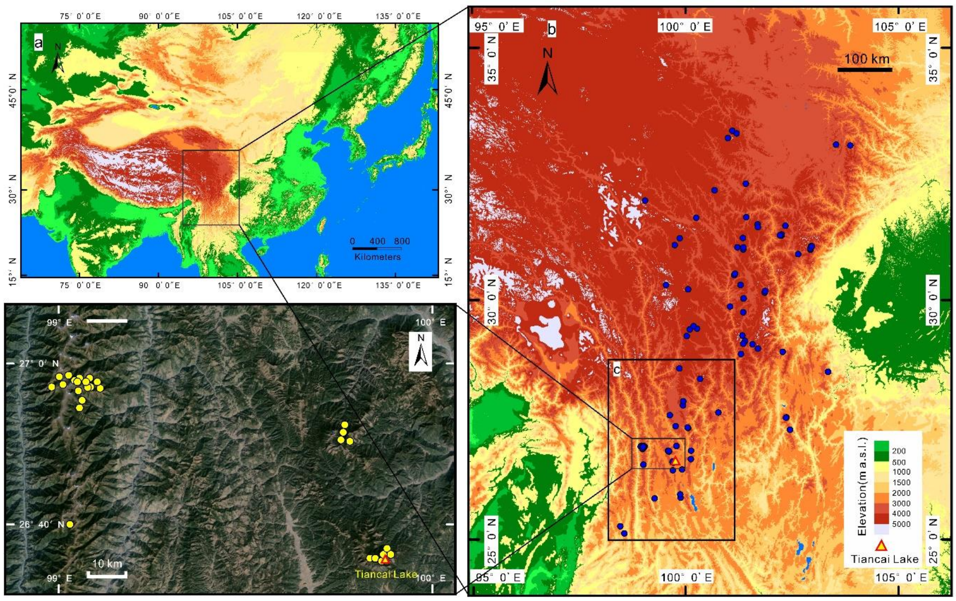

Fig. 1 Map of south-west China (a) showing the location of 100 lakes included in full calibration training set (square box). The subset of 47 lakes from Yunnan province is shown in the square box (b). The triangle (△) indicates the location of Tiancai Lake in (c).

Clim. Past Discuss., doi:10.5194/cp-2016-96, 2016
Manuscript under review for journal Clim. Past
Published: 4 October 2016

Climate of the Past
Discussions

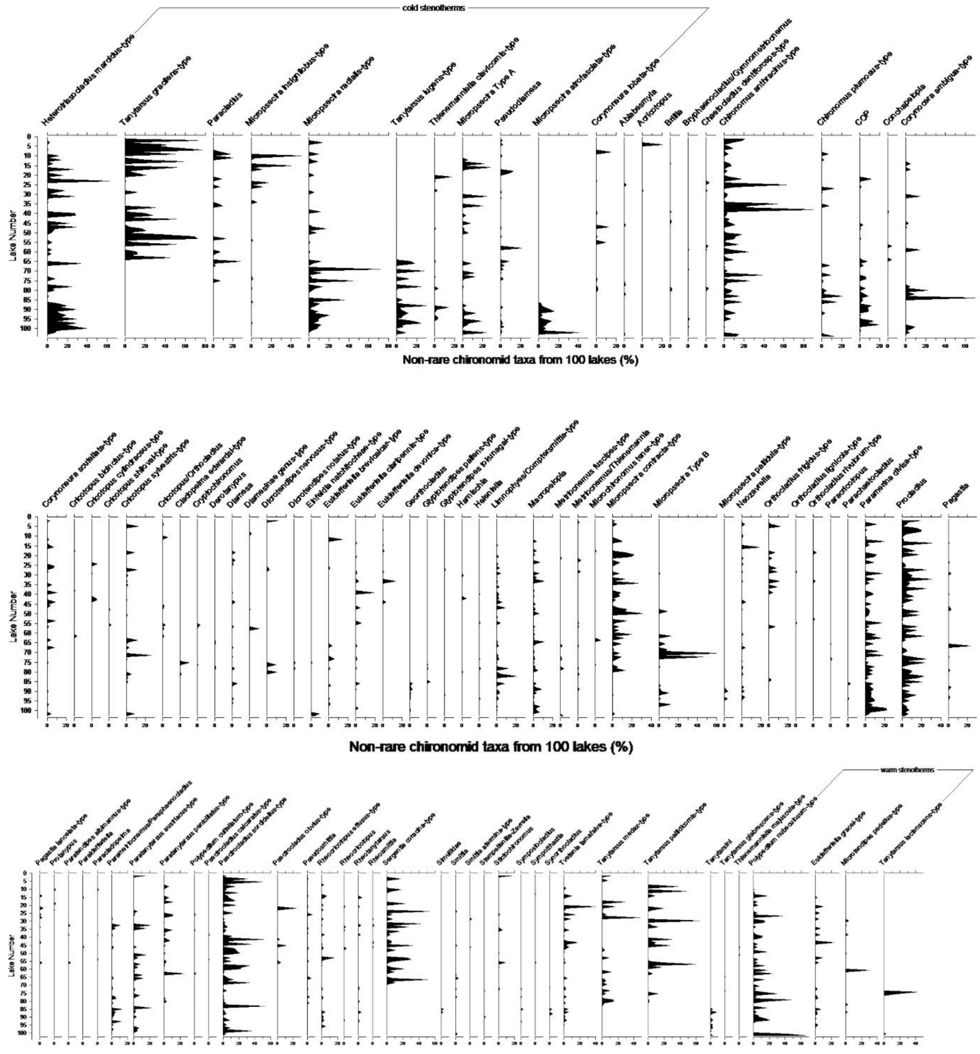

Fig 2a. Chironomid species percent diagram of 95 non-rare taxa with N and N2 > 2. Lake number from 1 to 100 is on the y-axis. Warm and cold stenotherms were identified and grouped based on optical observation and the canonical correspondence analysis (CCA) species scores.

Clim. Past Discuss., doi:10.5194/cp-2016-96, 2016
Manuscript under review for journal Clim. Past
Published: 4 October 2016

Fig 2b. Forty-one (41) non-rare chironomid species present in the short core (28 cm) from Tiancai Lake.

Clim. Past Discuss., doi:10.5194/cp-2016-96, 2016
Manuscript under review for journal Clim. Past
Published: 4 October 2016

Climate of the Past
Discussions

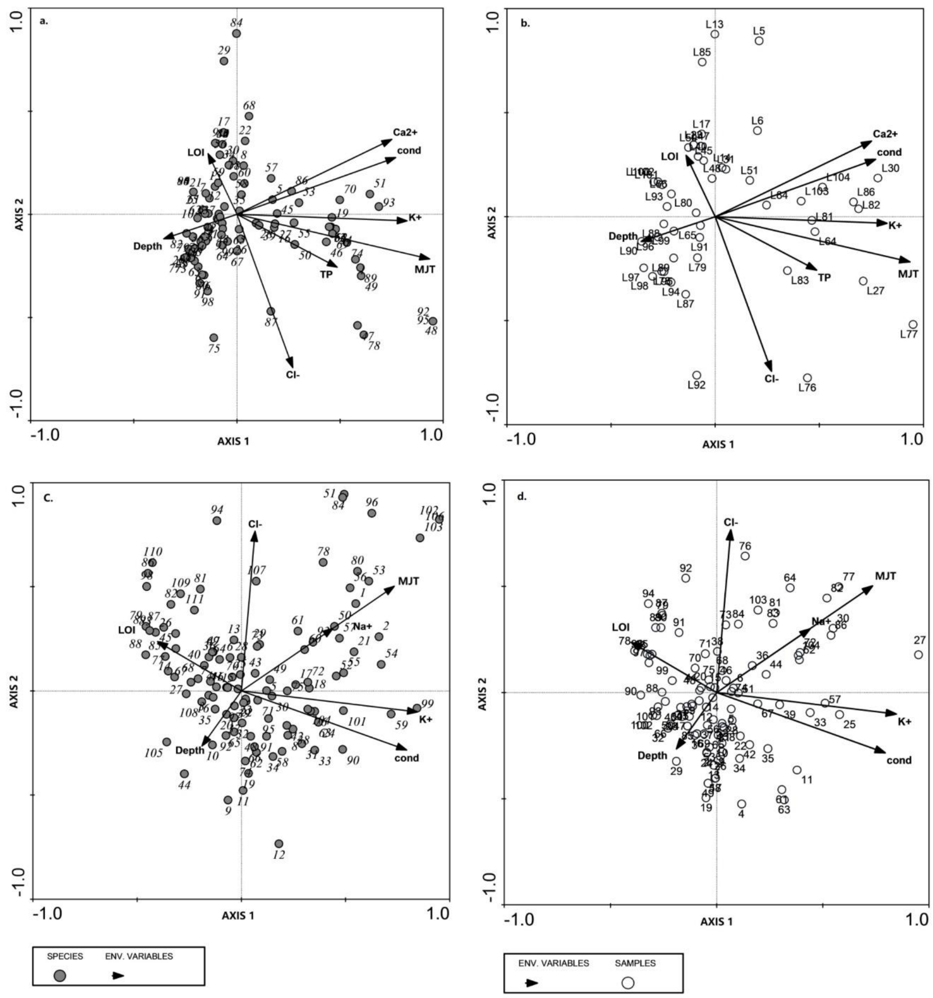

Fig 3 CCA bip-lots of sample and species scores constrained to environmental variables that individually explain a significant ($p < 0.05$) proportion of the chironomid species data. (a) species and (b) sample scores constrained to eight significant environmental variables in the 47 Yunnan lakes training set. (c) species and (d) sample scores constrained to seven significant variables in the 100 lakes of southwestern China. The species codes are correspondent to the taxa names shown in Fig. 2a.

Clim. Past Discuss., doi:10.5194/cp-2016-96, 2016
Manuscript under review for journal Clim. Past
Published: 4 October 2016

Climate of the Past
Discussions

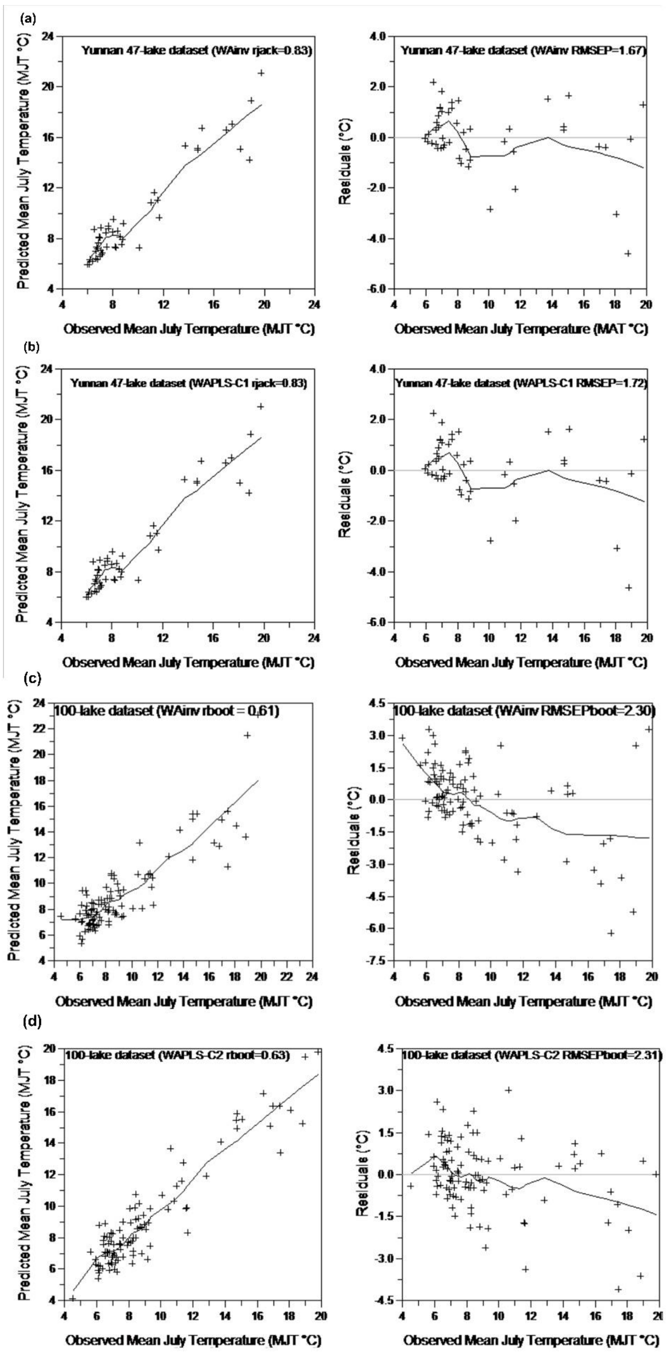

Fig 4 Performance of the weighted average models with inverse deshrinking (WAinv) and partial least square (WA-PLS) models using the 47 lakes and 100 lakes calibration data sets: (a) WAinv jackknifed model with 47 lakes (b) WA-PLS jackknifed

Clim. Past Discuss., doi:10.5194/cp-2016-96, 2016
Manuscript under review for journal Clim. Past
Published: 4 October 2016

Climate of the Past Discussions

model with 47 lakes (c) WAinv bootstrapped model with 100 lakes and (d) WA-PLS bootstrapped model with 100 lakes. Diagrams on the left show the predicted versus observed mean July temperature (MJT) and diagrams on the right display residuals of the predicted versus observed mean July temperature. Note that all the models have a tendency to over-predict temperatures from the cold end of the gradient and underestimate temperatures at the warm end. This is typical for the WA based models.

Clim. Past Discuss., doi:10.5194/cp-2016-96, 2016
Manuscript under review for journal Clim. Past
Published: 4 October 2016

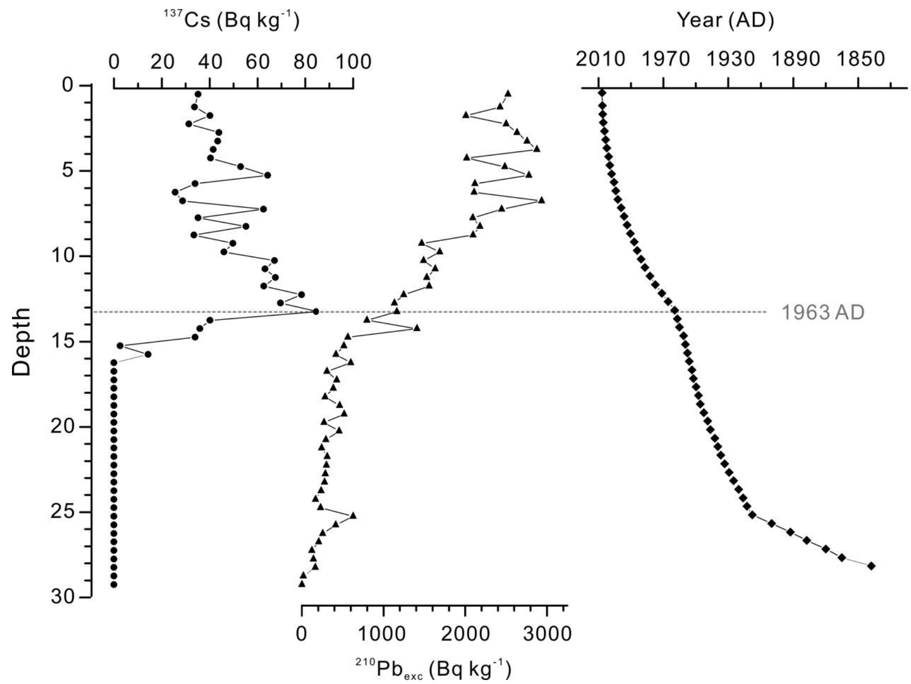

Fig 5 The age and depth model for ^{210}Pb dating results of the short core (30 cm) from Tiancai Lake. The concentration of ^{137}Cs (circle), excess ^{210}Pb (triangle) and the calibrated age (AD years) (square) were plotted against core sample depth, respectively.

Clim. Past Discuss., doi:10.5194/cp-2016-96, 2016
Manuscript under review for journal Clim. Past
Published: 4 October 2016

Climate of the Past
Discussions

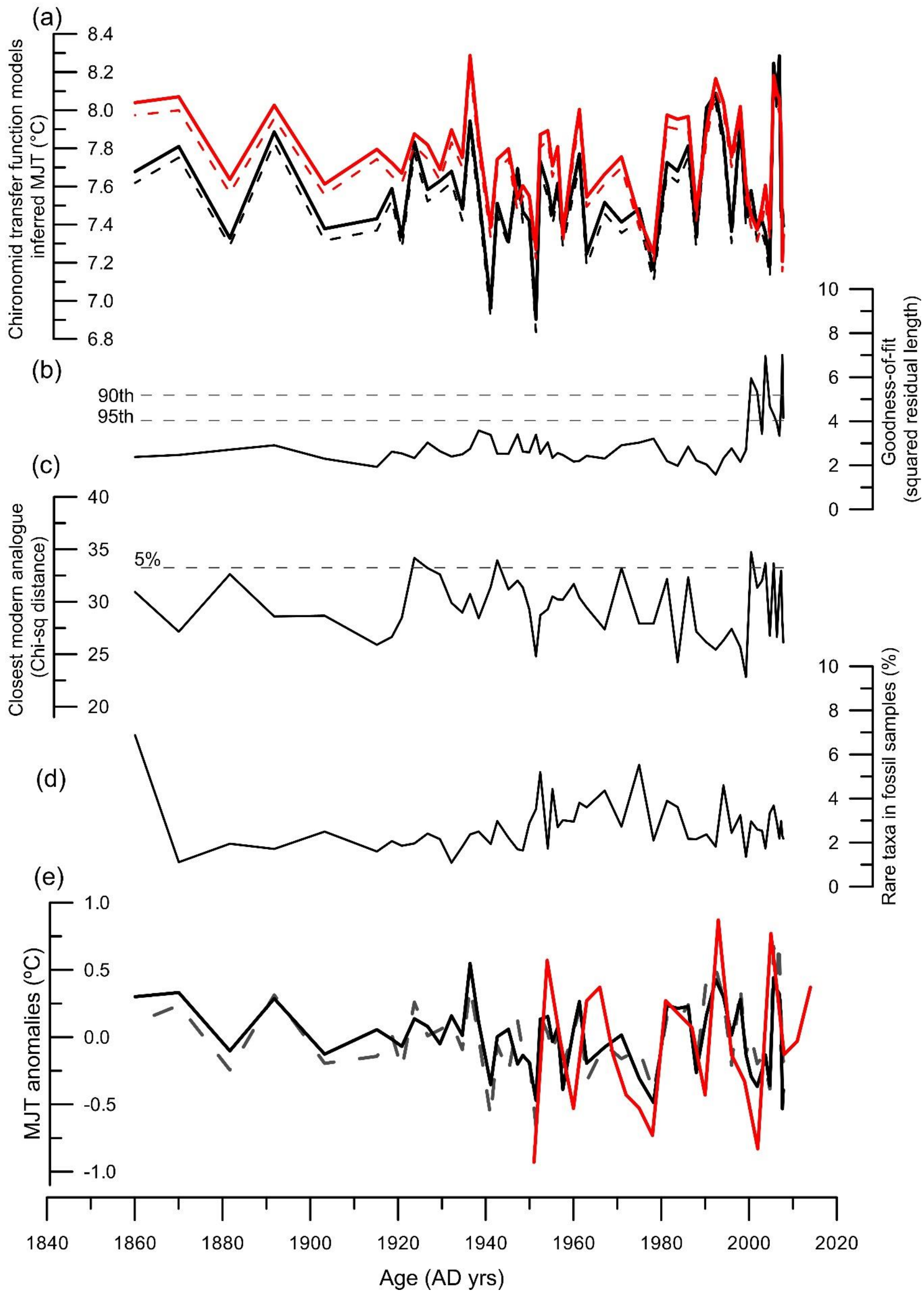

Fig 6 (a) Chironomid-based mean July temperature reconstruction results from Tiancai Lake based on 4 transfer function models: solid red line is the reconstruction based on the weighted average partial least square (WAPLS) bootstrapped model with 2 components using 100 lakes calibration set, solid black line is the

Clim. Past Discuss., doi:10.5194/cp-2016-96, 2016
Manuscript under review for journal Clim. Past
Published: 4 October 2016

Climate of the Past Discussions

reconstruction based on the WAPLS jackknifed model with 1 component using 47 lakes in Yunnan, dashed black line is based on the weighted average with inverse deshrinking (WAinv) jackknifed model using 47 lakes in Yunnan and dashed red line is based on WAinv jackknifed model using 100 lakes in southwestern China.
Reconstruction of diagnostic statistics for the 100 lake dataset where (b) displays the goodness-of-fit statistics of the fossil samples with mean July temperature (MJT). Dashed lines are used to identify samples with 'poor fit' (> 95th percentile) and 'very poor fit' (> 90th percentile) with temperature (c) Nearest modern analogues for the fossil samples in the calibration data set, where dashed line is used to show fossil samples with 'no good' (5%) modern analogues. (d) Percentage of chironomid taxa in fossil samples that are rare in the modern calibration data set (N < 2 and N2 < 2). (e) Comparison between the chironomid-based transfer function reconstructed trends with the instrumental data from Lijiang weather station (in red solid line, with three-sample moving average). Black solid line represents the reconstruction based on the WAPLS bootstrapped model with 2 components using 100 lakes calibration set and grey dashed line represents the reconstruction based on the WAPLS bootstrapped model with 1 component using 47 lakes calibration set from Yunnan in this diagram.

Clim. Past Discuss., doi:10.5194/cp-2016-96, 2016
Manuscript under review for journal Clim. Past
Published: 4 October 2016

Climate of the Past Discussions

Table 1. List of all the 18 environmental and climate variables measured from southwestern Chinese lakes, with mean, minimum and maximum values cited for the 47 lakes calibration set from Yunnan and the full 100 lakes, respectively.

Variable	**Unit**	**Symbol**	**Mean (47 lakes)**	**Min (47 lakes)**	**Max (47 lakes)**	**Mean (100 lakes)**	**Min (100 lakes)**	**Max (100 lakes)**
Altitude	m	alt	3534	1769	4506	3785	1769	4608
Mean July precipitation	mm	MJP	500	174	721	392	104	1055
Mean annual precipitation	mm	MAP	2171	731	3156	1820	505	5228
Mean July temperature	°C	MJT	9.7	6	19.8	9.1	4.2	19.8
Secchi depth	m	SD	2.7	0.4	11	3.5	0.2	12.5
Conductivity	µm cm^{-1}	Cond	40.6	5	234	55.8	5	336
Total dissolved solids	mg L^{-1}	TDS	15.8	2.5	70.3	18.4	1.9	79.7
pH	-	pH	8.3	7.23	10	8.5	7.23	10
Depth	m	Depth	8.2	0.5	40	10.7	0.25	52
Total Nitrogen	mg L^{-1}	TN	0.4	0.01	3.4	0.3	0.01	3.4
Total Phosphorus	mg L^{-1}	TP	0.07	0	1.6	0.05	0	1.6
Sodium	mg L^{-1}	Na+	2.9	0.23	37.2	2.7	0.22	37.2
Potassium	mg L^{-1}	K+	0.5	0	4.5	0.5	0	4.5
Magnesium	mg L^{-1}	Mg^{2+}	2.2	0.2	20	2.2	0	20
Calcium	mg L^{-1}	Ca^{2+}	5.4	0.8	28.7	7.3	0.8	34.6
Chlorine	mg L^{-1}	Cl-	2.4	0	9	1.7	0	9
Sulfate	mg L^{-1}	SO42-	2.3	0.1	8.7	3.9	0.1	31.6
Loss-on-ignition	%	LOI	32.1	1.92	77.1	24.3	1.92	77.1

Clim. Past Discuss., doi:10.5194/cp-2016-96, 2016
Manuscript under review for journal Clim. Past
Published: 4 October 2016

Table 2. CCA summary of the eight significant variables ($p < 0.05$) including canonical co-efficients and t-values of the environmental variables with the ordination axes including (a) 47 lakes and 53 non-rare species and (b) 100 lakes and 95 non-rare species

2a

	Axis 1	Axis 2	Axis 3	Axis 4
Eigenvalues	0.43	0.19	0.15	0.12
Cum % var. spp.	14.6	21.1	26.1	30.2
Cum% var. spp. – env. relation	37.7	54.5	67.3	77.8

Variable	**Total variance explained**	**Regression/canonical coefficients**		**t-values of regression coefficients**	
		Axis 1	**Axis 2**	**Axis 1**	**Axis 2**
cond	10.7%	-0.03	0.06	-0.24	0.19
depth	4.4%	-0.18	-0.02	-3.62	-0.14
TP	4.7%	0.09	-0.01	1.76	-0.04
K+	10.7%	0.32	0.25	4.36	1.32
Ca2+	9.9%	0.32	0.84	2.71	2.72
Cl-	5.5%	0.01	-0.54	0.16	-3.81
MJT	16.0%	0.44	-0.75	4.95	-3.19
LOI	3.7%	0.06	0.34	1.11	2.84

2b

	Axis 1	Axis 2	Axis 3	Axis 4
Eigenvalues	0.24	0.17	0.10	0.08
Cum % var. spp.	5.90	10.0	12.5	14.6
Cum% var. spp. - env. relation	33.5	57.0	71.2	82.7

Variable	**Total variance explained**	**Regression/canonical coefficeints**		**t-values of regression coefficients**	
		Axis 1	**Axis 2**	**Axis 1**	**Axis 2**
cond	4.4%	0.44	-0.27	3.99	-2.65
depth	2.0%	-0.15	-0.21	-1.90	-2.82
Na+	2.7%	0.10	0.02	0.91	-0.17
K+	4.8%	0.49	-0.07	4.67	-0.65
Cl-	3.4%	-0.21	0.65	-2.18	6.94
MJT	4.4%	0.14	0.62	1.49	6.90
LOI	3.1%	-0.09	0.04	-1.02	0.48

Clim. Past Discuss., doi:10.5194/cp-2016-96, 2016
Manuscript under review for journal Clim. Past
Published: 4 October 2016

Table 3. Partial Canonical Correspondence Analysis (pCCA) result with environmental variables that showed a significant correlation ($p < 0.05$) in CCAs with chironomid species data included, where (a) is based on the 47 lakes training set, where mean July temperature (MJT) (bold) is the only variable retained its significance level ($p < 0.01$) after each pCCAs and (b) is based on the 100 lakes training set in which depth, K+, Cl-, LOI and MJT (bold) retained their significance ($p < 0.01$) after each step of the pCCAs.

a.

Variable	**Covariable**	**% var. axis 1**	**% var. axis 2**	**p-value**	**λ1**	**λ2**	**λ1/λ2**
cond	none	10.7	11.5	0.001	0.317	0.340	0.927
	TP	10.4	11.5	0.001	0.290	0.320	0.898
	K+	6.30	11.7	0.001	0.168	0.310	0.540
	MJT	6.00	17.7	0.001	0.154	0.300	0.508
	Cl-	11.0	10.4	0.001	0.308	0.290	1.055
	LOI	11.3	11.7	0.001	0.322	0.340	0.961
	Depth	9.80	12.0	0.001	0.278	0.340	0.820
	Ca2+	4.40	12.8	0.010	0.119	0.340	0.348
	ALL	6.40	10.3	0.001	0.125	0.200	0.628
depth	none	4.40	14.4	0.004	0.131	0.430	0.307
	cond	3.50	12.8	0.032	0.092	0.340	0.271
	TP	4.30	13.4	0.005	0.121	0.370	0.324
	MJT	3.70	13.1	0.017	0.096	0.340	0.286
	Cl-	4.80	14.7	0.002	0.134	0.410	0.324
	LOI	4.60	14.8	0.005	0.133	0.420	0.316
	K+	4.20	12.6	0.005	0.111	0.340	0.331
	Ca2+	3.80	12.8	0.011	0.101	0.340	0.295
	ALL	4.70	10.4	0.006	0.089	0.200	0.447
K+	none	10.7	11.4	0.001	0.316	0.340	0.932
	Ca2+	6.50	11.4	0.001	0.175	0.300	0.576
	cond	6.30	11.7	0.001	0.167	0.310	0.537
	MJT	3.90	13.1	0.013	0.099	0.340	0.292
	Cl-	10.4	10.2	0.001	0.292	0.290	1.025
	LOI	10.8	11.4	0.001	0.309	0.330	0.948
	Depth	10.4	11.8	0.001	0.296	0.340	0.884
	TP	9.20	12.1	0.001	0.258	0.340	0.761
	ALL	6.50	10.2	0.001	0.127	0.200	0.638
TP	none	5.70	13.8	0.004	0.170	0.410	0.414
	K+	4.20	12.8	0.011	0.112	0.340	0.330

Clim. Past Discuss., doi:10.5194/cp-2016-96, 2016
Manuscript under review for journal Clim. Past
Published: 4 October 2016

	cond	5.40	12.2	0.008	0.143	0.320	0.443
	Ca2+	5.70	12.1	0.001	0.152	0.320	0.471
	Cl-	5.60	14.6	0.008	0.157	0.410	0.383
	LOI	5.90	14.3	0.004	0.169	0.410	0.413
	Depth	5.60	13.2	0.008	0.159	0.370	0.425
	MJT	3.60	13.1	0.071	0.091	0.340	0.267
	ALL	5.10	10.4	0.014	0.097	0.200	0.487
Cl-	none	5.50	15.6	0.001	0.163	0.470	0.351
	Ca2+	5.90	10.5	0.001	0.158	0.280	0.566
	cond	5.80	11.0	0.001	0.154	0.290	0.527
	K+	5.20	10.8	0.001	0.138	0.290	0.484
	MJT	5.20	9.80	0.001	0.134	0.250	0.530
	LOI	5.00	16.3	0.005	0.144	0.460	0.310
	Depth	5.90	14.5	0.001	0.166	0.410	0.401
	TP	5.40	14.6	0.002	0.151	0.410	0.368
	ALL	4.30	10.5	0.014	0.082	0.200	0.412
LOI	none	3.70	15.9	0.036	0.11	0.470	0.234
	TP	3.90	14.6	0.022	0.109	0.410	0.267
	cond	4.30	12.7	0.008	0.115	0.340	0.343
	K+	3.90	12.3	0.019	0.103	0.330	0.316
	MJT	4.00	12.8	0.008	0.103	0.330	0.312
	Cl-	3.20	16.6	0.082	0.091	0.460	0.196
	Depth	3.90	14.9	0.017	0.111	0.420	0.264
	Ca2+	4.20	12.7	0.004	0.114	0.340	0.337
	ALL	4.80	10.4	0.006	0.091	0.200	0.457
Ca2+	none	9.90	11.6	0.001	0.293	0.350	0.847
	TP	9.90	11.5	0.001	0.276	0.320	0.854
	COND	3.60	12.9	0.040	0.095	0.340	0.278
	K+	5.70	11.5	0.001	0.152	0.300	0.500
	MJT	5.30	11.2	0.001	0.138	0.290	0.479
	Cl-	10.3	9.90	0.001	0.289	0.280	1.036
	LOI	10.4	11.8	0.001	0.297	0.340	0.879
	Depth	9.30	12.0	0.001	0.264	0.340	0.772
	ALL	5.90	10.3	0.003	0.115	0.200	0.578
MJT	**none**	**16.0**	**8.70**	**0.001**	**0.394**	**0.340**	**1.159**
	TP	**11.3**	**12.1**	**0.001**	**0.316**	**0.340**	**0.929**
	COND	**8.70**	**11.4**	**0.001**	**0.231**	**0.303**	**0.762**
	K+	**6.70**	**12.7**	**0.001**	**0.177**	**0.339**	**0.522**
	Ca2+	**8.90**	**10.8**	**0.001**	**0.239**	**0.288**	**0.830**

Clim. Past Discuss., doi:10.5194/cp-2016-96, 2016
Manuscript under review for journal Clim. Past
Published: 4 October 2016

Climate of the Past Discussions
Open Access
EGU

	Cl-	**13.0**	**9.00**	**0.001**	**0.365**	**0.253**	**1.443**
	LOI	**13.5**	**25.1**	**0.001**	**0.387**	**0.330**	**1.173**
	Depth	**12.7**	**11.8**	**0.001**	**0.359**	**0.336**	**1.068**
	ALL	**5.40**	**10.4**	**0.001**	**0.104**	**0.199**	**0.523**

b.

Variable	**Covariable**	**% var. axis 1**	**% var. axis 2**	**p-value**	**λ1**	**λ2**	**λ1/λ2**
cond	none	4.40	7.90	0.001	0.179	0.317	0.560
	depth	4.60	7.90	0.001	0.181	0.315	0.570
	Na+	4.10	7.70	0.001	0.159	0.305	0.520
	K+	1.80	8.20	0.004	0.069	0.316	0.220
	Cl-	4.60	7.50	0.001	0.179	0.293	0.610
	MJT	3.60	8.10	0.001	0.140	0.313	0.450
	LOI	3.60	7.90	0.001	0.140	0.310	0.450
	ALL	1.70	7.60	0.016	0.057	0.259	0.220
depth	**none**	**2.00**	**9.80**	**0.001**	**0.082**	**0.397**	**0.210**
	cond	**2.20**	**8.10**	**0.002**	**0.083**	**0.315**	**0.260**
	Na+	**2.10**	**9.90**	**0.001**	**0.083**	**0.387**	**0.210**
	K+	**2.20**	**8.30**	**0.001**	**0.083**	**0.321**	**0.260**
	Cl-	**2.00**	**10.0**	**0.002**	**0.079**	**0.390**	**0.200**
	MJT	**2.00**	**9.60**	**0.001**	**0.077**	**0.371**	**0.210**
	LOI	**2.10**	**9.50**	**0.001**	**0.082**	**0.372**	**0.220**
	ALL	**2.20**	**7.60**	**0.001**	**0.074**	**0.259**	**0.290**
Na+	none	2.70	9.60	0.001	0.111	0.388	0.290
	Cond	2.40	7.80	0.001	0.091	0.305	0.300
	depth	2.80	9.80	0.001	0.112	0.387	0.290
	K+	2.30	7.70	0.001	0.089	0.296	0.300
	Cl-	2.70	8.90	0.001	0.106	0.347	0.310
	MJT	1.90	9.60	0.008	0.072	0.371	0.190
	LOI	2.40	9.60	0.001	0.093	0.375	0.250
	ALL	1.70	7.70	0.011	0.058	0.259	0.220
K+	**none**	**4.80**	**7.90**	**0.001**	**0.192**	**0.322**	**0.600**
	cond	**2.10**	**8.20**	**0.002**	**0.082**	**0.316**	**0.260**
	Na+	**4.30**	**7.60**	**0.001**	**0.171**	**0.296**	**0.580**
	Cl-	**5.00**	**7.40**	**0.001**	**0.195**	**0.290**	**0.670**
	LOI	**4.10**	**8.20**	**0.001**	**0.160**	**0.320**	**0.500**
	Depth	**4.90**	**8.10**	**0.001**	**0.193**	**0.321**	**0.600**
	MJT	**3.30**	**8.20**	**0.001**	**0.129**	**0.314**	**0.410**
	ALL	**2.00**	**7.70**	**0.003**	**0.069**	**0.259**	**0.270**

Cl-	**none**	**3.40**	**9.70**	**0.001**	**0.137**	**0.393**	**0.350**
	cond	**3.50**	**7.60**	**0.001**	**0.137**	**0.293**	**0.470**
	K+	**3.60**	**7.60**	**0.001**	**0.140**	**0.290**	**0.480**
	MJT	**3.20**	**8.60**	**0.001**	**0.125**	**0.332**	**0.380**
	LOI	**3.50**	**9.40**	**0.001**	**0.137**	**0.366**	**0.370**
	Depth	**3.40**	**9.90**	**0.001**	**0.134**	**0.390**	**0.340**
	Na+	**3.40**	**8.80**	**0.001**	**0.132**	**0.347**	**0.380**
	ALL	**2.80**	**7.60**	**0.001**	**0.098**	**0.259**	**0.380**
LOI	**none**	**3.10**	**9.30**	**0.001**	**0.124**	**0.377**	**0.330**
	Na+	**2.70**	**9.60**	**0.001**	**0.107**	**0.375**	**0.290**
	cond	**2.20**	**8.00**	**0.001**	**0.086**	**0.310**	**0.280**
	K+	**2.40**	**8.30**	**0.001**	**0.092**	**0.320**	**0.290**
	MJT	**3.00**	**9.30**	**0.001**	**0.116**	**0.361**	**0.320**
	Cl-	**3.20**	**9.40**	**0.001**	**0.124**	**0.366**	**0.340**
	Depth	**3.10**	**9.40**	**0.001**	**0.124**	**0.372**	**0.330**
	ALL	**2.20**	**7.60**	**0.001**	**0.074**	**0.259**	**0.290**
MJT	**none**	**4.40**	**9.10**	**0.001**	**0.176**	**0.371**	**0.470**
	Na+	**3.50**	**9.40**	**0.001**	**0.137**	**0.371**	**0.370**
	cond	**3.50**	**8.10**	**0.001**	**0.137**	**0.313**	**0.440**
	K+	**2.90**	**8.20**	**0.001**	**0.113**	**0.314**	**0.360**
	LOI	**4.30**	**9.20**	**0.001**	**0.168**	**0.361**	**0.470**
	Cl-	**4.20**	**8.50**	**0.001**	**0.164**	**0.332**	**0.490**
	Depth	**4.30**	**9.40**	**0.001**	**0.171**	**0.371**	**0.460**
	ALL	**2.70**	**7.50**	**0.001**	**0.091**	**0.259**	**0.350**

Clim. Past Discuss., doi:10.5194/cp-2016-96, 2016
Manuscript under review for journal Clim. Past
Published: 4 October 2016

Climate of the Past Discussions Open Access EGU

Table 4. Results of the transfer function development where (a) shows the performance of the weighted average model with inverse and classical deshrinking (WAinv, WAcla), weighted average partial least squares (WA-PLS) models for reconstructing mean July temperature using (a) 47 lakes from Yunnan and 53 non-rare chironomid species and (b) for using 100 lakes from south-western China and 95 non-rare chironomid species. The bold indicates the models that are tested for reconstructing the mean July temperatures from Tiancai Lake.

a.

	Model type	RMSE	R2	Ave_Bias	Max_Bias	Jack_R2	Jack_Ave_Bias	Jack_Max_Bias	RMSEP
1	**WA_Inv**	**1.27**	**0.90**	**1.61E-15**	**1.73**	**0.83**	**0.113**	**2.83**	**1.67**
2	WA_Cla	1.34	0.90	1.25E-15	2.14	0.83	0.119	2.60	1.65
C1	**WAPLS**	**1.27**	**0.90**	**-0.039**	**1.75**	**0.83**	**0.109**	**3.15**	**1.72**
C2	WAPLS	0.82	0.96	0.035	1.73	0.81	0.194	3.57	1.78
C3	WAPLS	0.62	0.98	-0.028	0.59	0.79	0.163	3.54	1.87

b.

#	Model type	RMSE	R2	Ave_Bias	Max_Bias	Boot_R2	Boot_Ave_Bias	Boot_Max_Bias	RMSE_s1	RMSE_s2	RMSEP
1	**WA_Inv**	**1.69**	**0.76**	**-6.07E-15**	**3.52**	**0.61**	**0.06**	**5.30**	**0.69**	**2.19**	**2.30**
2	WA_Cla	1.93	0.76	-9.43E-15	3.37	0.61	0.07	4.78	0.86	2.20	2.36
c1	WAPLS	1.69	0.76	-0.064	3.47	0.60	0.023	5.28	0.71	2.22	2.33
c2	**WAPLS**	**1.23**	**0.88**	**0.052**	**1.91**	**0.63**	**0.101**	**5.16**	**0.89**	**2.14**	**2.31**
c3	WAPLS	1.05	0.91	-0.026	1.56	0.60	0.065	5.08	1.03	2.19	2.41